J. Phys. B: Atom. Molec. Phys., Vol. 10, No. 16, 1977. Printed in Great Britain.

Electron-impact cross sections for Cu atoms†

S Trajmar, W Williams and S K Srivastava
Jet Propulsion Laboratory, California Institute of Technology, 4800 Oak Grove Drive, Pasadena, California 91103, USA

Received 22 April 1977

Abstract. Relative differential electron-impact cross sections have been measured for elastic scattering for excitation of the $3d^{10}4p\ ^2P_{1/2,3/2}$, $3d^94s^2\ ^2D_{5/2}$ and $3d^94s^2\ ^2D_{3/2}$ states of Cu at 6, 10, 20, 60 and 100 eV in the 0° to 140° angular range. The relative values were normalised to the absolute scale by utilising He as a secondary standard for determining the correct energy dependence and by accepting the value of the calculated elastic differential cross section at 100 eV, 40° as $1{\cdot}28 \times 10^{-16}$ cm^2 sr^{-1}. Integral and momentum-transfer cross sections have been obtained by extrapolation to 180°. The cross section for the excitation of the ^2P state is large compared to that for elastic scattering, and population inversion in this state with respect to the ^2D state is readily achieved by electron impact. None of the theoretical predictions utilising classical, Born or static-exchange approximations agree with the experimental results at low impact energies.

1. Introduction

A number of metal vapours have been suggested as excellent media for efficient, high-power lasers (Petrash 1971). These predictions are based mainly on the energy level schemes of the metal atoms. No information has been available, however, on the electron-impact excitation cross sections for the laser levels or for other levels which influence the behaviour of the laser systems. The main reason for the absence of information in this area is due to the difficulty which one encounters in trying to carry out quantitative measurements or reliable calculations.

One of the metal-vapour lasers which has been widely studied and has demonstrated a high efficiency and scalability is Cu. No experimental electron-collision data existed on Cu prior to our recent measurements (Williams and Trajmar 1974). Theoretical calculations were carried out by Leonard (1967) (Gryzinsky's method) and Trainor *et al* (1975) (impact-parameter method) for the ^2P and ^2D excitations. Ormande (1974 private communication) performed some preliminary close-coupling calculations on the electron-impact excitation of the $^2D_{5/2}$ level. More recently Winter *et al* (1975) and Winter (1977) carried out scattering calculations with the static-exchange and Born models.

In this report we summarise our electron-impact cross-section measurements on Cu for elastic scattering, for excitation of the upper and lower laser levels (^2P and ^2D respectively) and for momentum transfer at 6, 10, 20, 60 and 100 eV energies.

† Work supported in part by the National Aeronautics and Space Administration Contract No NAS7-100 and in part by the US Energy Research and Development Administration Order No LS-76-26.

The normalisation of all experimental data was achieved by accepting the 40° differential elastic cross section at 100 eV as calculated by Winter (1977), and by calibrating the energy dependence of the Cu cross section against He. The results are presented in tables 1 and 2 and in figures 5–11.

2. Experimental procedure

The experimental apparatus used in the present measurements consist of an electron gun, hemispherical energy selector and analyser, electrostatic tube lenses, an electron detector and the source for the Cu beam. The Cu beam is generated by heating a tantalum crucible, containing copper, by electron bombardment. The vapour effuses through a 0·75 mm diameter and 3 mm long hole and is crossed with the energy-selected electron beam of the required impact energy E_0 at 90° angle. Electrons scattered at a given scattering angle θ into a small solid angle ($\sim 10^{-3}$ sr) are detected as a function of energy loss utilising pulse-counting and multichannel-scaling techniques. The instrument and the experimental procedure have previously been described in more detail (Williams and Trajmar 1974, Chutjian 1974). Representative energy-loss spectra are shown in figures 1 and 2.

The energy-loss spectra obtained at fixed impact energies and scattering angles constitute the basic information: the relative scattering intensities associated with the various processes. The scattering intensities are related to the corresponding cross section by the following relation:

$$N_e = k\sigma(\theta) \int_V \int_\Omega F_e n \, d\Omega \, dV \tag{1}$$

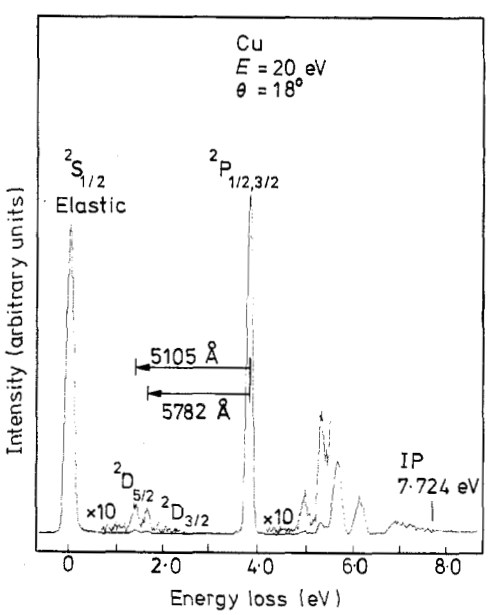

Figure 1. Energy-loss spectrum of Cu. The elastic peak, the upper and lower laser levels and transitions are shown.

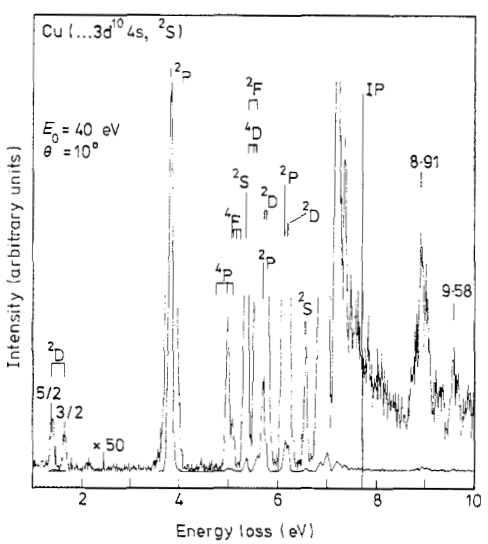

Figure 2. Energy-loss spectrum of Cu showing the higher energy-loss region.

where N_e is the number of electrons per second scattered by the entire interaction volume V and detected at a scattering angle θ over a solid angle of acceptance Ω. F_e and n are the electron flux and the target density distributions respectively and k is the overall instrumental efficiency factor. The cross section has been assumed to be independent of angle over the acceptance angle of the detector and represents an average cross section within the angular resolution of the instrument. (For detailed discussion see Srivastava *et al* 1975). In taking relative intensities from a given energy-loss spectrum, all the geometrical and efficiency factors cancel and one obtains the relative cross sections. Also, at a given impact energy the change of scattering geometry with scattering angle can be minimised and approximately accounted for, and relative cross sections in the same arbitrary units are obtained.

The major problem is the transformation of the relative cross sections to absolute cross sections. The straightforward method of determining all the parameters relating the scattering intensities to the corresponding cross sections is not feasible. Other methods previously used for normalisation encounter difficulties in connection with metal vapours, especially at temperatures required to vaporise the less volatile elements like Cu. Phaseshift analysis of an accurately measured angular distribution is not feasible partly because the cross sections are, in general, very forward peaked (requiring many partial waves in the analysis and very accurate low-angle scattering measurements), and partly because many inelastic channels open up at low energies. Normalisation to total cross sections (determined by recoil or electron transmission measurements) is prevented by the lack of such data. Theoretical calculations at the present time are not accurate enough at low impact energies to serve as standards.

At the present time, one of the most reliable normalisation procedures is to carry out the elastic intensity measurements for the species in question against He. Elastic cross sections for He are known and they can serve as standards for calibration if the relative target densities of the two gases are known. This procedure has been successfully used with permanent gases and is described in detail by Srivastava *et al* (1975). However, this procedure is not suitable for the metal vapours mainly due to difficulties associated with the determination of metal atom densities in a beam. To overcome these difficulties we have devised a four-stage calibration procedure which is described in the following:

(i) In the first stage the angular distribution of the elastic scattering is determined at a given impact energy and corrected for the angle dependence of the geometry against He and N_2. The elastic cross sections are obtained in this way at 6, 10, 20, 60 and 100 eV in *arbitrary units which are different at every energy.*

(ii) The second stage consists of collecting energy-loss spectra and determining the relative inelastic to elastic intensity ratios at each impact energy and angle. The result of this procedure is inelastic cross sections in the same arbitrary units as the corresponding elastic cross sections.

(iii) In the third stage relative elastic scattering intensities from the Cu beam and from a He beam with nearly identical scattering geometry are determined at 20° scattering angle as a function of incident energy between 6 eV and 100 eV. The geometry is indicated in figure 3. The He and Cu scattering geometry should be most similar at 0° scattering angle; however, at this angle the direct electron beam cannot be distinguished from the elastically scattered electrons. A compromise angle of 20° has been chosen. The measured intensity ratios at various impact energies are proportional to the corresponding elastic cross sections

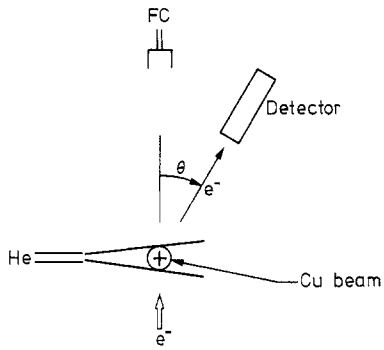

Figure 3. Collision geometry for He calibration.

$$\left[\frac{I_{Cu}(E_0)}{I_{He}(E_0)}\right]_{\theta=20^\circ} = C\,\frac{\rho_{Cu}}{\rho_{He}}\left[\frac{DCS_{Cu}(E_0)}{DCS_{He}(E_0)}\right]_{\theta=20^\circ} \tag{2}$$

The proportionality factors are the target densities (ρ) and the relative geometrical factor (C). The assumption made here is that the factor C is independent of E_0. The target density was kept constant during the measurement of the elastic scattering intensity of Cu at the various impact energies by regulating and monitoring the power of the electron bombardment heating and by repeating the measurements several times. The He density was kept constant by keeping the gas pressure behind the effusion orifice constant. The result of this procedure is a set of elastic 20° differential cross sections as the function of impact energy *all in the same arbitrary units.* Utilising these cross sections and the relative elastic and inelastic differential and integral cross sections (which we determined at specific impact energies in stage (ii), we obtained *all cross sections in the same arbitrary units at all energies.*

(iv) The fourth stage of normalisation consists of finding a cross section (either elastic or inelastic) differential or integral at a given energy and angle or energy respectively and obtaining the single factor C (ρ_{Cu}/ρ_{He}) needed to normalise the arbitrary unit to the absolute scale. We pursued both experimental and theoretical approaches in this fourth stage and will discuss them briefly in the following.

The experimental approach is based on the use of the generalised oscillator strength for an electron-impact excitation process which has been defined by Bethe (1930) as

$$f^{G}_{0n}(K) = \frac{W}{2}\frac{k_0}{k_n}K^2\,DCS^{B}_{0n}(K) \tag{3}$$

where W is the excitation energy, k_0 and k_n are momenta of the electron before and after collision, K is the momentum transfer, and $DCS^{B}_{0n}(K)$ is the Born cross section. It is easy to show that the generalised oscillator strength converges to the optical f value at zero momentum transfer. One can retain the form of equation (3) and define the apparent generalised oscillator strength by replacing the Born cross section by the experimentally determined true cross section. It has been shown by Lassettre and Dillon (1969) that the apparent generalised oscillator strength at zero momentum transfer is also equal to the optical f value:

$$\lim_{K\to 0}\left[f^{G}_{0n}(K)\right]_{exp} \to f^{opt}_{0n}. \tag{4}$$

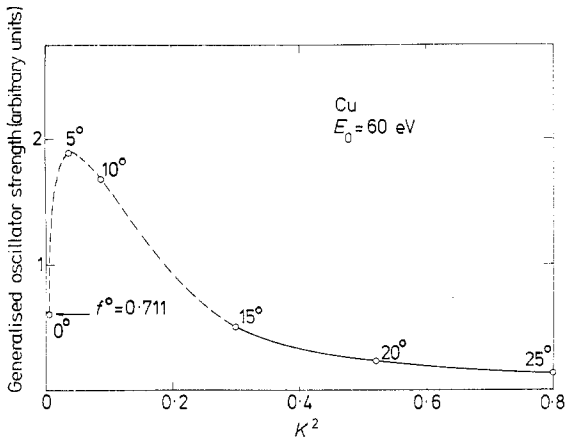

Figure 4. Generalised oscillator strengths calculated from the experimental ^2P differential cross sections at 60 eV impact energy. The 15° value represents the last reliable experimental point. The broken curve indicates a possible extrapolation to zero momentum transfer.

Since the optical f value for the resonance $^2S \rightarrow {}^2P$ transition is known for Cu, a normalisation could be achieved by requiring the generalised oscillator strengths calculated from the experimental ^2P differential cross sections to converge to the proper f_{0n}^{opt} value ($f_{0n}^{opt} = 0{\cdot}711$ from Corliss 1970). Serious uncertainties arise, however, in connection with this extrapolation at low and intermediate impact energies as demonstrated in figure 4. The measurements have large uncertainties at angles below 15° due to geometrical and background effects and in addition, the curve changes rapidly making the extrapolation uncertain. At impact energies of 100 eV or higher, we would expect that this procedure will give a fairly reliable calibration point, but the low signal level in the inelastic channel, coupled with other experimental problems prevented us from carrying out accurate measurements at these high energies.

The theoretical methods are most reliable at high impact energies. The static-exchange calculations of Winter (1977) seem to be the most reliable calculations at the present time on electron–Cu elastic scattering. For reasons discussed below we have accepted the value of the calculated elastic 40° differential cross section at 100 eV ($1{\cdot}28 \times 10^{-16}$ cm^2 sr^{-1}) and normalised our experimental data to this point.

3. Results and discussion

The differential cross sections for elastic scattering and for the excitation of the ^2P and ^2D states are shown in figures 5–9 and are listed in table 1. The angular behaviours are as expected in general: forward peaking for the elastic scattering and for the ^2P excitation, nearly isotropic for the ^2D excitation, and increasing forward peaking character with increasing impact energies. The elastic DCS show the oscillation characteristic of heavy elements. The angular dependence curves serve as much more rigorous checks for the theoretical models than the integral cross sections alone and from a practical point of view they are important because they determine the momentum-transfer cross sections.

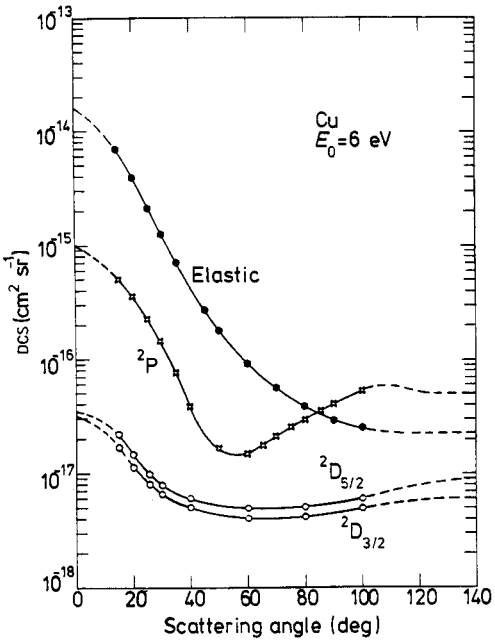

Figure 5. Differential cross sections at 6 eV impact energy.

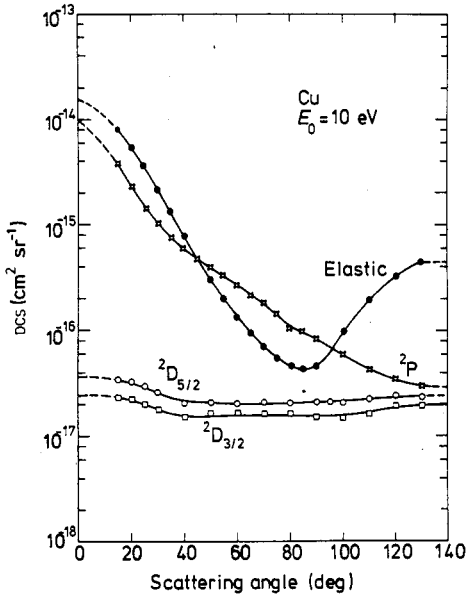

Figure 6. Differential cross sections at 10 eV impact energy.

In Figure 9 the 100 eV elastic differential cross sections of the present experiment are compared with the theoretical calculations. The calculations of Winter utilise the static-exchange model and those of Fink and Ingram (1972) use relativistic Hartree–Fock–Slater potentials without exchange.

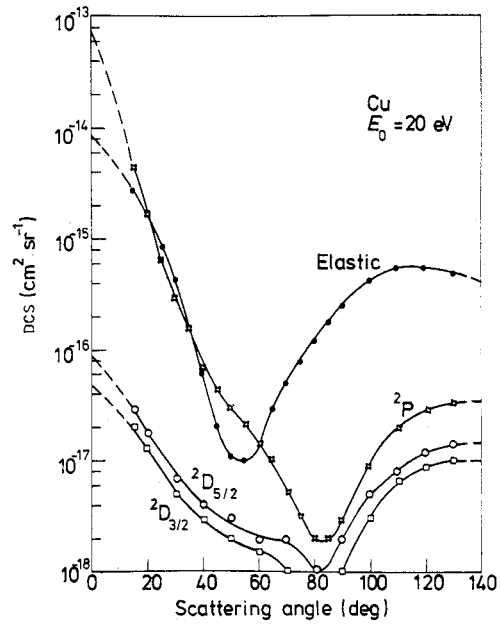

Figure 7. Differential cross sections at 20 eV impact energy.

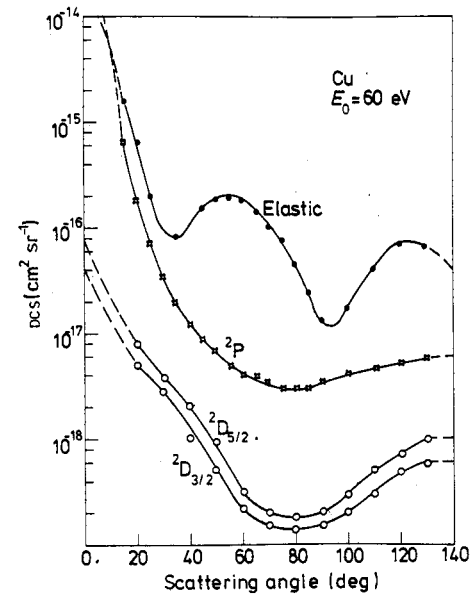

Figure 8. Differential cross sections at 60 eV impact energy.

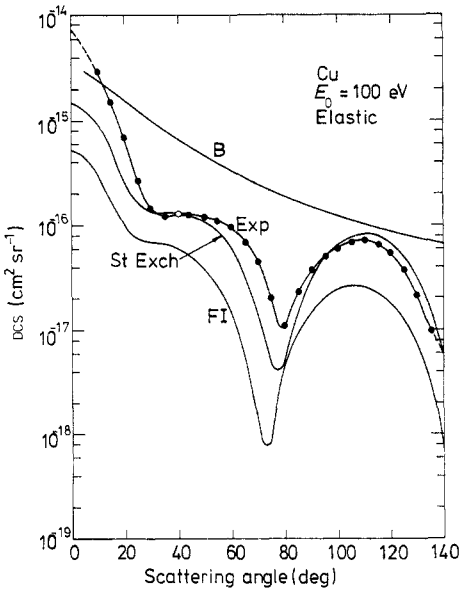

Figure 9. Differential cross sections at 100 eV impact energy. B Born approximation. St Exch: static-exchange calculation (Winter 1977). Exp: present experimental results. FI: Hartree–Fock–Slater calculation (Fink and Ingram 1972).

The shape of the experimental DCS compares favourably with both calculations, but the calculations differ by a factor of two in absolute magnitude. Our experimental data was normalised to the static-exchange model calculations of Winter (1977). The static-exchange model is expected to give quite reliable cross sections at 100 eV. Indeed, it was found that the calculated elastic differential cross section curve agreed quite well with the shape of the experimentally determined angular distribution. The very low-angle theoretical cross sections are expected to be low because polarisation effects are neglected. The 40° cross section should have only a small influence from these effects. Furthermore, the cross sections around 40° are nearly angle independent. These considerations and the fact that the calculated curve is in good agreement with the experimental shape makes the 40° point a natural choice for normalisation.

The integral cross sections are shown in figures 10 and 11 and summarised in tables 2 and 3. In the elastic case (figure 10) neither the Born nor the static-exchange model agrees with the experiment. The two models converge to each other as the energy increases and the experimental value is between the two theoretical values, but the convergence expected at high energies has not yet occurred at 100 eV. The experimental value at 100 eV is closer to the Born prediction, but this must be fortuitous in the light of the bad agreement in the DCS (figure 9). The static-exchange value at 100 eV is about a factor of three smaller than the experimental one. This discrepancy is partly due to the omission of polarisation effects. If one corrects the calculated low-angle DCS to follow the experimental shape below 40°, the value of the calculated integral cross section increases from 9·4 to 15·4 $\times$ 10^{-16} cm^2.

For the resonance ^{2}P excitation ($J = \frac{1}{2}$ and $\frac{3}{2}$ levels are not resolved) the Born predictions are the closest to the experimental values. The classical calculation of Leonard (1967) and the impact-parameter calculation of Trainor *et al* (1975) indicate values which are lower than the Born results, but even the Born results are lower

than the experimental ones except at very low energies. All theoretical methods predict cross sections for the ^2D excitation which are lower than the present results at energies above 10 eV, but peak at energies closer to threshold than the experimental curves. It is interesting to note that the inelastic momentum transfer at 6 and 10 eV impact energies are as important as the corresponding elastic momentum transfers.

The accurate estimation of errors associated with the present cross sections is very difficult, but on the basis of careful examination of the various error sources and our previous experience in cross-section measurements and normalisations, we believe that the cross sections are correct to about a factor of two in absolute value and to about $\pm 30\%$ in relative value.

In our previous publication (Williams and Trajmar 1974) the 20 and 60 eV cross sections were normalised to the calculated Born integral elastic cross sections at those energies. Those cross sections should be multiplied by a factor of 0·54 at 20 eV and 0·41 at 60 eV to bring them into agreement with the present results. (The angular behaviours are naturally not affected.) Trainor *et al* (1975) suggested on the basis of their calculations that our previous 20 and 60 eV cross sections should be lowered

Table 1. Differential cross sections for electron-impact excitation of Cu. The low- and high-angle data separated from the rest by horizontal lines are extrapolated values.

	DCS (10^{-16} cm^2 sr^{-1})							
	E_0 = 6 eV				E_0 = 10 eV			
θ(deg)	Elastic	^2P	$^2D_{5/2}$	$^2D_{3/2}$	Elastic	^2P	$^2D_{5/2}$	$^2D_{3/2}$
0	160	10·1	0·35	0·32	159	93	0·36	0·24
5	131	8·6	0·33	0·29	132	72	0·36	0·24
10	98	6·8	0·27	0·23	106	52	0·35	0·23
15	68·4	5·15	0·23	0·17	80·3	38·4	0·35	0·23
20	38·4	3·69	0·15	0·11	53·0	22·5	0·33	0·23
25	20·4	2·25	0·10	0·08	34·8	14·1	0·30	0·20
30	12·4	1·46	0·08	0·07	21·6	10·1	0·26	0·18
35	7·28	0·77	—	—	13·2	7·41	—	—
40	4·29	0·39	0·06	0·05	7·73	6·00	0·21	0·15
45	2·69	—	—	—	4·68	4·80	—	—
50	1·82	0·17	—	—	2·96	3·98	0·21	0·17
55	—	—	—	—	1·94	3·35	—	—
60	0·95	0·15	0·05	0·04	1·32	2·64	0·21	0·17
65	—	0·18	—	—	0·98	2·12	—	—
70	0·57	0·21	—	—	0·71	1·77	0·21	0·17
75	—	0·26	—	—	0·56	1·46	—	—
80	0·41	0·29	0·05	0·04	0·47	1·02	0·21	0·17
85	—	0·35	—	—	0·44	0·98	—	—
90	0·29	0·41	—	—	0·45	0·81	0·21	0·15
100	0·26	0·54	0·06	0·05	0·98	0·59	0·21	0·15
110	—	—	—	—	1·89	0·44	0·23	0·17
120	0·23	0·51	0·08	0·06	3·14	0·35	0·24	0·20
130	0·23	0·51	0·09	0·06	4·46	0·29	0·24	0·20
140	0·23	0·51	0·09	0·06	4·46	0·29	0·24	0·20
160	0·23	0·51	0·09	0·06	4·46	0·29	0·24	0·20
180	0·23	0·51	0·09	0·06	4·46	0·29	0·24	0·20

Table 1. (continued)

	DCS (10^{-16} cm^2 sr^{-1})								
	E_0 = 20 eV				E_0 = 60 eV				100 eV
θ(deg)	Elastic	^{2}P	^{2}D$_{5/2}$	^{2}D$_{3/2}$	Elastic	^{2}P	^{2}D$_{5/2}$	^{2}D$_{3/2}$	Elastic
0	86·3	798	0·84	0·48	180	490	0·77	0·44	71·1
5	62·6	366	0·68	0·36	114	191	0·44	0·26	48·3
10	41·0	158	0·45	0·27	51·8	48·5	0·20	0·12	29·6
15	27·9	43·5	0·29	0·20	15·8	6·54	—	—	15·2
20	17·0	17·0	0·18	0·13	6·54	1·80	0·08	0·05	6·90
25	8·46	6·65	—	—	2·07	0·71	—	—	2·69
30	4·23	2·85	0·07	0·05	0·98	0·35	0·04	0·03	1·41
35	1·58	1·52	—	—	0·81	0·20	—	—	1·21
40	0·60	0·78	0·04	0·03	1·10	0·12	0·02	0·01	1·28
45	0·21	0·44	—	—	1·53	0·09	—	—	1·24
50	0·11	0·30	0·03	0·02	1·91	0·07	0·01	0·005	1·21
55	0·10	0·21	—	—	2·01	0·05	—	—	1·07
60	0·13	0·14	0·02	0·02	1·85	0·04	0·003	0·002	0·97
65	0·29	0·10	—	—	1·47	0·04	—	—	0·66
70	0·50	0·05	0·02	0·01	1·04	0·04	0·002	0·002	0·45
75	0·78	0·03	—	—	0·77	0·03	—	—	0·20
80	1·22	0·02	0·01	0·01	0·47	0·03	0·002	0·002	0·11
85	1·76	0·02	—	—	0·24	0·03	—	—	0·23
90	2·48	0·03	0·02	0·01	0·13	0·04	0·002	0·002	0·38
100	4·23	0·09	0·05	0·03	0·18	0·04	0·003	0·002	0·59
110	5·27	0·20	0·08	0·07	0·42	0·04	0·005	0·003	0·72
120	5·37	0·29	0·12	0·09	0·71	0·05	0·007	0·005	0·55
130	4·77	0·32	0·14	0·10	0·66	0·05	0·01	0·005	0·21
140	4·05	0·33	0·14	0·10	0·41	0·06	0·01	—	0·06
160	4·05	0·33	0·14	0·10	0·38	0·09	0·01	0·005	0·34
180	4·05	0·33	0·14	0·10	0·38	0·10	0·01	0·005	0·85

by a factor of seven. The present results, however, indicate that lowering by only a factor of two is necessary.

Recently, before the completion of our present normalisation procedure, we normalised our relative measurements at 60 eV to the static-exchange calculation. They were presented in a report (Trajmar *et al* 1977). To transform the cross sections

Table 2. Integral and momentum-transfer cross sections in units of 10^{-16} cm^2.

E_0(eV)	6	10	20	60	100
Q(elastic)	4·95	84·3	49·4	23·9	29·04
Q(^{2}P)	8·85	40·8	44·3	17·7	—
Q(^{2}D$_{5/2}$)	1·05	2·85	0·90	0·15	—
Q(^{2}D$_{3/2}$)	0·75	2·10	0·75	0·11	—
Q^M(elastic)	71·1	38·1	45·9	7·20	5·71
Q^M(^{2}P)	7·35	17·0	7·80	1·35	—
Q^M(^{2}D$_{5/2}$)	1·05	2·85	0·90	0·06	—
Q^M(^{2}D$_{3/2}$)	0·90	2·25	0·75	0·05	—

Table 3. Comparison of integral cross sections.

	E_0(eV)	6	10	20	60	100
$Q_{00}(10^{-16}\,cm^2)$	Present	49·5	84·3	49·4	23·9	16·0
	Born[a]	—	173·0	121·0	58·9	39·4
	St Exch[b]	44·1	17·6	5·7	7·7	9·4
	Exp[c]	—	—	91	59	—
$Q_{2p}(10^{-16}\,cm^2)$	Present	8·85	40·8	44·3	17·7	—
	Born[a]	30·8	31	23·5	9·2	—
	Trainor[d]	5·3	8·7	8·7	5·3	—
	Exp[c]	—	—	72·7	36·5	—
$Q_{^2D_{5/2}}(10^{-16}\,cm^2)$	Present	1·05	2·85	0·90	0·15	—
	Leonard[e]	2·2	1·2	0·21	0·014	—
	Ormande[f]	0·4	0·16	0·04	—	—

[a,b] Winter (1977).
[c] Williams and Trajmar (1974), same data as the present results but normalised to Born calculation.
[d] Trainor *et al* (1975).
[e] Leonard (1967).
[f] Ormande (1974 private communication).

given in this report to the more accurate present values, one has to multiply them by a factor of 1·5.

In figure 2 the energy-loss spectrum of Cu is shown up to 10 eV. Several transitions below the ionisation limit have significant cross sections which contribute to the $3d^{10}4p\ ^2P$ and $3d^94s^2\ ^2D$ level populations by cascade and influence the process of energy deposition. Discrete features associated with autoionising states are present

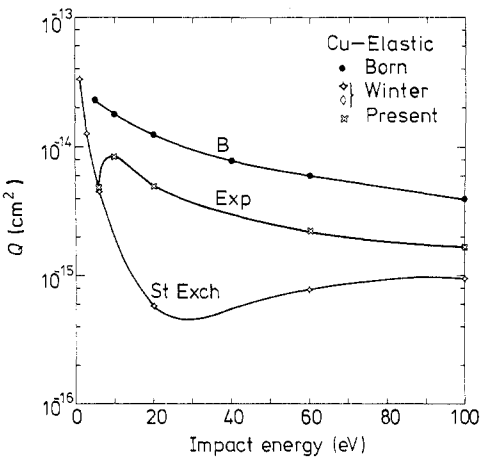

Figure 10. Integral elastic cross sections; B: Born approximation; St Exch: static exchange calculations (Winter 1977); Exp: present experimental results.

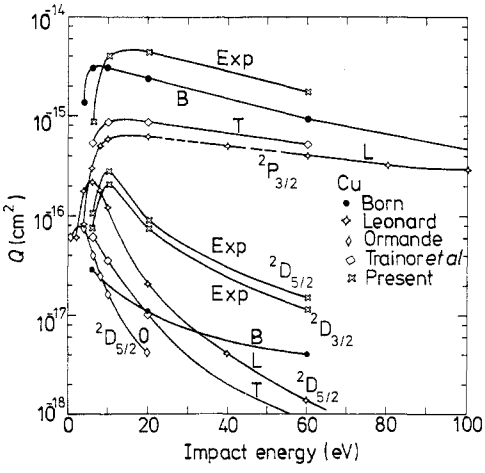

Figure 11. Integral excitation cross sections for the ^2P and ^2D states; B: Born approximation (Winter 1977); T: impact-parameter theory (Trainor *et al* 1975); L: classical Gryzinsky model (Leonard 1967); O: close-coupling calculation (Ormande 1974); Exp: present experimental results. For the ^2P level, the $\frac{3}{2}$ and $\frac{1}{2}$ components are not separated except for the curve L.

above the ionisation limit and are the major contributors to the overall ionisation process. In an accurate modelling of the Cu-vapour laser these transitions should also be considered.

Acknowledgment

We are grateful to N W Winter for sending us the results of his calculations prior to publication and for valuable discussions.

References

Bethe H A 1930 *Ann. Phys., Lpz* **5** 325
Chutjian A 1974 *J. Chem. Phys.* **61** 4279
Corliss C H 1970 *J. Res. NBS* A **74** 781
Fink M and Ingram J 1972 *Atom. Data* **4** 129
Lassettre E N and Dillon M A 1969 *J. Chem. Phys.* **50** 1829
Leonard D A 1967 *IEEE J. Quantum Electron.* **3** 380
Petrash G G 1971 *Usp. Fiz. Nauk.* **105** 645
Srivastava S K, Chutjian A and Trajmar S 1975 *J. Chem. Phys.* **63** 2659
Trainor D, Mandl A and Hyman H 1975 March–August *Metal Vapor Visible Laser Kinetic Program, Semi-Annual Tech. Rept* Avco Everett Research Laboratories Incorporated
Trajmar S, Williams W and Srivastava S K 1977 *Final Report, Part 3, Copper Laser Research* (Prepared for Los Alamos Scientific Laboratory by G Russel, Jet Propulsion Laboratory, Pasadena, California)
Williams W and Trajmar S 1974 *Phys. Rev. Lett.* **33** 197
Winter N W 1977 to be published
Winter N W, Cartwright D C and Wary M M 1975 *Proc. 9th Int. Conf. on Physics of Electronic and Atomic Collisions* vol 2 (Seattle: University of Washington Press) Abstracts p 1023